A New Adaptive Multiscale Morphological Filter and Robust RVFLN Classifier for Distributed Generation Systems during Islanding and Non-Islanding Events

N. R. Nayak, P. K. Dash, B. N. Sahu, and Ranjeeta Bisoi

Siksha O Anusandhan Deemed to be University, Bhubaneswar, Odisha, India
pkdash.india@gmail.com

Abstract: A new method for islanding and non-islanding disturbances detection and classification is proposed for a multiple PV based distributed generation (DG) system utilizing adaptive multi-scale morphological filter (AMF) and random vector functional link network (RVFLN) classifier. In comparison to different signal analysis techniques, the mathematical MF, that has wide application in power signals, EEG signal analysis, image processing, pattern recognition, etc. posses the benefit of easy execution, fast processing, and minimal computations. Further it is well known that a single scale morphological filter has limited noise filtering capacity and may also filter useful signal disturbance components resulting in erroneous detection of disturbance signals in microgrid. Therefore, an adaptive multiscale combined morphological filter is presented in this paper built on the concept of multiscale overall filtering which has better denoising effect and can retain useful signals better than the traditional filter. The proposed technique is built upon the measurement of voltage signal samples and the processing of these signals through AMF has been done for feature extraction. The extracted features are then employed as inputs to an efficient, fast, and easily implementable randomized network based classifier (RVFLN) which is made robust to reject the presence noise and outliers in the signal data. The outputs exhibited from the suggested technique concludes that it is s very fast and accurate technique for the detection and classification of islanding and non-islanding events in comparison to the widely used approaches.

Index Terms: Microgrid, RRVFLN, Adaptive Multi-scale Morphological Filter (AMF), Pattern Recognition, Islanding, and Non-islanding Disturbances.

1. Introduction

The utilization of renewable energy sources have been raising day by day because they can serve electricity near to the customer premises. Previously, the power has been generated in a bulk amount and transmitted via long distance transmission lines to the customers. But while using this traditional technique, there are many problems occurs. The main problem is the transmission loss and also the size of the generation system. To overcome these difficulties, the use of distributed generation (DGs) systems has been implemented. Distribution generation systems are much more reliable and efficient than traditional ones. There are many sources of electricity that have been used now a day's such as, solar, wind, fuel cells, biomass, geothermal etc. Thus these DGs are very useful to solve the environmental problems using these renewable sources. In any microgrid, an islanding condition occurs if the DG continues to supply the power to the loads/network without the main utility supply. Islanding condition will be very harmful for field workers. Due to islanding the voltage and frequency of the signal transferred to the customer side will change which can damage the equipments used by the users. Thus, it becomes important to detect islanding as soon as it occurs. In another way, we can say that the DG should be rigged with an anti-islanding prevention or loss of mains protection which needs to catch the loss from the grid and should trip the connected DG from the grid. As per IEEE standard 1547, the islanding should be detected within 0.2sec. To maintain the safety all the DGs should operate only when the utility supply is present. Uncertainties associated with islanding and non-islanding events occurring on a microgrid pose certain challenges that may require dynamic thresholding

Received: October 23th, 2019. Accepted: July 13rd, 2020
DOI: 10.15676/ijeei.2020.12.3.6

for the events both during islanding and grid connected modes. Threshold selection is a huge challenge in case of islanding operation due to non detection zone.

For islanding detection, in literature, there have been found many techniques. It can be passive, active or communication based techniques. There are many active techniques used in the literature, such as, automatic phase shift [1], voltage drift [2], voltage unbalance and total harmonic distortion [3], Sandia frequency shift [4,5], negative sequence voltage [6], impedance measurement [7], energy of rate of change of voltage phase angle and frequency and its rate of change [8,9], bilateral reactive power variation [10] and so on. Active method is basically a small injection of perturbation which creates a vast change when there is islanding [11,12,13]. These techniques are beneficial because they have less non detection zone. But these techniques carry some demerits such as, system instability; power quality deterioration; also the performance reduces for multiple DG based systems. Here, this paper focuses on the passive methods. Passive methods can be frequency domain methods or time domain methods. Pattern recognition based methods are also considered as passive methods. Different frequency domain methods found in literature like rate of change of frequency relay and rate of change of phase angle difference relay [14], S-Transform [15,16], wavelet transform [17] to extract the frequency domain patterns. These rate of change of phase angle difference relay and rate of change of frequency relay methods give good results when the difference between the loads and the generation is significant. But when the difference is less the accuracy of these methods deteriorates. To reduce the non detection zone the signal processing methods WT, ST [18,19] have been introduced. A new cross-correlation anti-islanding detection technique has been introduced by Voglitsis et al [20]. Comparison of the signal processing techniques provided in [15,21] for islanding event. Also a passive islanding detection technique by WPT is given in [22]. Different pattern recognition techniques have been compared by Faqhruldin et al. [23] for islanding detection.

Further different non-islanding disturbances like voltage swells, voltage sags, capacitor switching, balanced / unbalanced load switching, different types of faults occur in the microgrid due to momentary interruptions, short-circuits, and power electronic converters (DC-DC converter and voltage source inverter) operations required for distributed generations (DG) integration. These disturbances assume significant importance during both islanding and grid synchronous operational modes [18, 19, and 21]. The islanding scenario contains serious challenges and therefore requires to be detected as early as possible (within 2 sec) to avoid instability and equipments burnout [18]. Further the threshold values for islanding and some of the above mentioned disturbances, detection depends significantly on DGs' operational modes [18]. Hence, the detection of both the islanding and non-islanding problems in microgrid is necessary to reduce the damages in various components. In recent years some new machine learning and signal decomposition techniques have been presented for islanding and non-islanding disturbance studies [19,24,25,39-43]. However, all the proposed approaches are fairly complex and their accuracy depends on the selection of filters, neurons, and their activation functions.

On the other hand, mathematical morphology [26-30] is a time domain signal processing method that uses only addition and subtraction for the calculations resulting in the reduction of the memory space and the detection time as well. Due to its simplicity and effectiveness it has extensive applications in different areas, like image processing, fault analysis in power systems, islanding detection in microgrids and vision detection, etc. Further it can be used to make translation matching and local correction of the original signal from front to back by constructing a certain structuring element (SE), and the morphological characteristics of the original signal are preserved while the noises are suppressed. In multiscale morphology, as a standard of measure, the structure element operator plays a major role in feature extraction from the shape of signals. Taking advantage of scale features of a structure element, signals can be decomposed into different scales in time zone. There are a multitude of shapes, such as flat SE, triangular SE, circular SE, semicircular SE, etc. Mathematical Morphology is less complex than WT and ST and has been used for the detection of passive islanding in [26]. In [26] the authors have used morphological wavelets for processing both islanding and non-islanding disturbance signals.

Although there are several machine learning based classifiers like decision tree, support vector machines, Adaptive fuzzy network systems, Artificial neural networks (ANN), randomized neural networks like ELM and RVFLN [31-34], etc., the RVFLN is found to be a superior candidate for pattern classification. It is a one layer feed forward neural network with direct link from input layer to output layer. The weights to inputs are assigned ranomly and pseudo inverse least square method is executed to compute the output weights. The architecture of RVFLN is very simple, learning speed is very fast and it also has good generalization performance which makes this model more efficient for both regression and classification tasks. The iterative tuning of weights is not required in case of RVFLN which may lead faster convergence, lesser training error and easy computation. Thus, in this work, a new integrated idea is designed for islanding and non-islanding disturbance detection and classification built on adaptive multi scale morphological filter (AMF) with a modified and improved version of the well known Random vector functional link network (RVFLN). Although the norm of the output weight is smaller in case of regularized RVFLN which may lead towards better generalization performance as compared to the conventional RVFLN, it suffers from the deterioration of the classification accuracy when the signal data contains outliers. Therefore to improve the regularized RVFLN performance a robust regularized weighted RVFLN known as RRVFLN is presented in this paper to reduce the impact of outliers. The existence of outliers may lead to unstability to the weight vector, thus it is required to update the weight vector. Thus smaller values to assign to the input patterns with higher training errors. The input patterns having higher training error are assigned with smaller weights and vice versa in order to decrease the impacts of outliers. Further AMF is an improved version of morphological filter (MF) where the structuring element has been made adaptive using water cycle optimization [35-37] for better results. Advantages of the suggested metaheuristic WCA technique are its fast global convergence within a few iterations and less computational complexity as compared to traditional DE, GA, PSO, etc., some suffer from premature convergence. The tracking signal is collected by using an AMF from where the features have been extracted to decide the threshold. The performance of the suggested method has been compared with recognized techniques to evaluate its superiority.

This structure of paper is organized in seven sections. Section 1 is the introduction and the background study of the proposed method. Section 2 describes the considered multiple DG based microgird model. Section 3 presents the proposed adaptive mathematical morphological filter (AMF) and the water cycle algorithm. Section 4 explains selected features. Section 5 presents the newly introduced RRVFLN structure. Section 6 describes the performance measures of the suggested technique. Finally, section 7 is followed by conclusion.

2. Application of the new filter in Multiple DG Based Microgrid

As stated in IEEE 1547 std. a microgrid system should work properly in both the modes, grid-connected mode and islanding mode, prior to effective power dispatch management. Non-islanding disturbances such as balanced load switching; unbalanced load switching, various types of faults have been generated in both the modes as a new contribution to literature. In any distributed generation based microgrid, the requirements for islanding detection capacity for the DGs are stated in UL1741. A four PV based IEEE 9-bus microgrid has been taken for the consideration and the model is given in Figure.1. In this microgrid system different other DGs have been used as well, such as, wind farm, Diesel Generators, Solid Oxide Fuel Cells, auxiliary Battery Energy Storage System, etc. But here in this paper mainly the PV penetration has been taken for the threshold detection. Table 1 presents the other description of the taken microgrid. In the microgrid model the islanding is attained by a utility connection switch s1. The DG based microgrid is created in MATLAB environment. The samples are studied under uniform sampling at 10kHz all the model generated voltage signal samples are passed through AMF to extract features. Table 2 describes the non-islanding disturbances generated in this microgrid model.

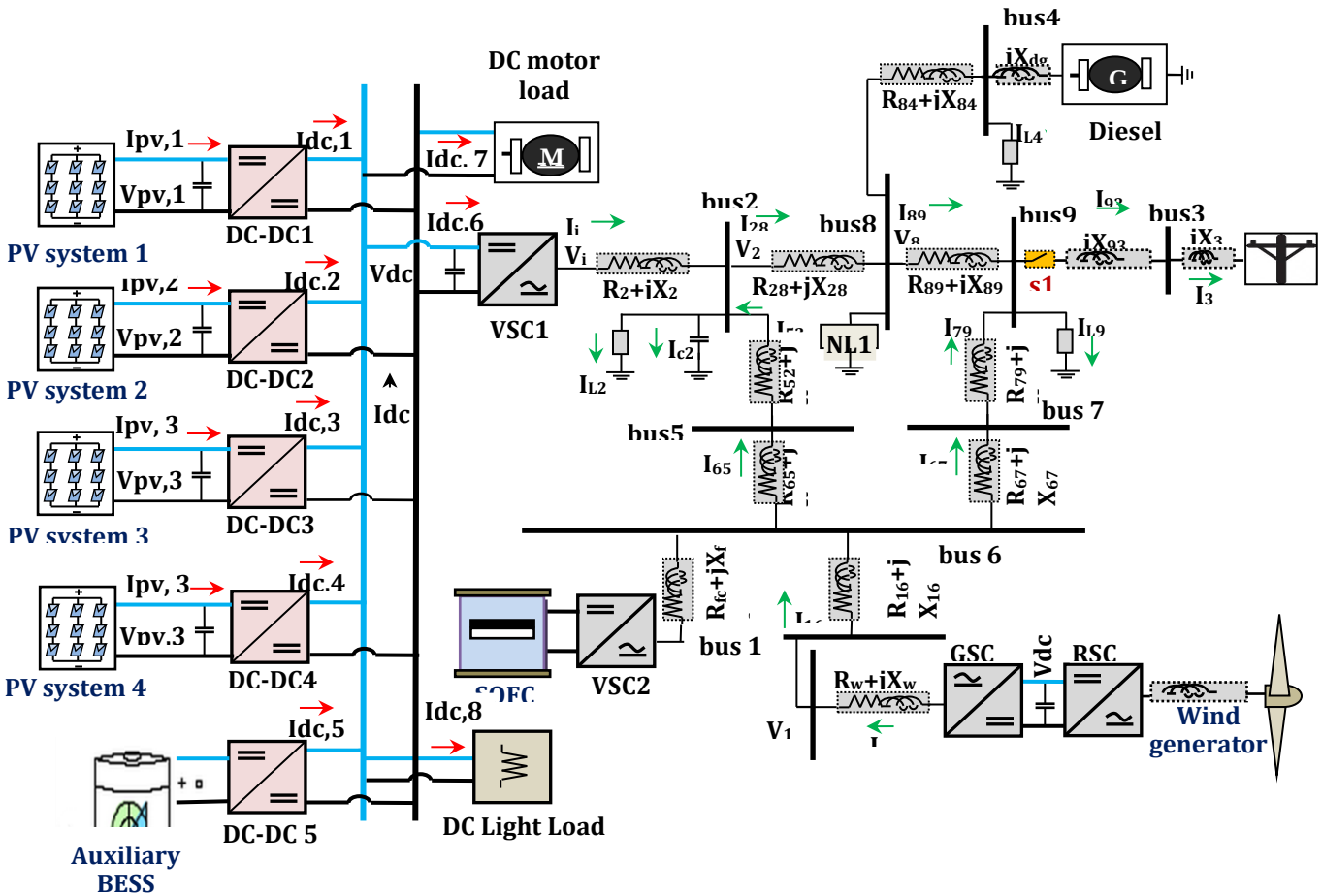

Figure 1. The taken Multi-DG based microgrid environment

Table 1. The microgrid system (with 9-bus multi-DG) parameters (IEEE std.)

Components	Data	Parameter values/km		
		R	*L*	*C*
DFIGURE (AC)	25 kV,1.5 MW 120 Volts	R_S=R_R=0.005 mΩ	--	31.841 nF
PV (DC)	400 kW, 500Volts	121 mΩ	0.97 mH	12.1 nF
Diesel generator	8.23 kW, 3.5 kVAR, 750 rpm	--	--	--
Turbine data	ρ=1.225 Kg/m^3, R_{bd} =58.6 m, ω_t =0.8, ω =1	--	--	--
Local load (bus 2)	100 kW, 5 kVAR	--	--	--
Local load (bus 9)	275 kW, 25 kVAR	--	--	--
R_w+jX_w	--	0.04 Ω	0.636 mH	--
R_{16}+jX_{16}	2.5 kms	0.074 Ω	2.61 mH	510 µF
R_2+jX_2	3.2 kms	0.0947 Ω	3.34 mH	--
jX_3 = jX_{93}	2 kms	0 Ω	2.08 mH	--
R_{84}+jX_{84} = R_{89}+jX_{89}	2.5 kms	0.074 Ω	2.61 mH	--
R_{65}+jX_{65}= R_{67}+jX_{67}	2 kms	0.0592 Ω	2.08 mH	--
R_{52}+jX_{52}= R_{79}+jX_{79}	4 kms	0.1184 Ω	4.17 mH	--
R_{28}+jX_{28}	5 kms	0.1332 Ω	4.69 mH	--
Filter capacitor (X_c)		--	--	52 mF
System operational frequency	50 Hz	--	--	--

Table 2. The microgrid generated disturbances (Islanding / non-islanding)

Different disturbances	Class(C)
Islanding (by opening the switch s1 in the microgrid model)	CI
Other Non-islanding disturbances	Class(C)
L Fault	CII
LL Fault	CIII
LLL Fault	CIV
Capacitor Switching	CV
Unbalanced Load switching	CVI
Balanced Load switching	CVII
Sudden voltage drop	CVIII

3. Adaptive Multi-scale Morphological Filter

The basic mathematical morphology is constructed using dilation, erosion, opening and closing operations. Say, S(n) = input signal, G(m)= structuring element, represented in F=(0, 1, …., N-1) and D=(0, 1, ….., M-1), respectively, where, (N>=M).

The mathematical expression of dilation and erosion are represented as:

$$D = (S \oplus G)(n) = \max\begin{cases} S(n-m) + G(n), \\ 0 \le (n-m) \le n, m \ge 0 \end{cases} \quad (1)$$

$$E = (S\Theta G)(n) = \min\begin{cases} S(n+m) + G(j), \\ 0 \le (n+m) \le n, m \ge 0 \end{cases} \quad (2)$$

The formulation of opening and closing depends on dilation and erosion. The mathematical representation can be represented as:

$$OP = (S \circ G)(n) = ((S\Theta G) \oplus G)(n) \quad (3)$$

$$CL = (S \bullet G)(n) = ((S \oplus G)\Theta G)(n) \quad (4)$$

where the operators $\oplus, \Theta, \circ$ and $\bullet$ refers to the dilation, erosion, opening and closing operations.

Morphological gradient filter can be obtained from the above expressions:

$$MG(n) = D(n) - E(n) = (S \oplus G)(n) - (S\Theta G)(n) \quad (5)$$

The above four operators are used in morphology to extract the signal features. Two different types of filters can be modeled using these operators such as open close and close open. There are another two filters can be represented using these four parameters, they are morphological median filter and multi-scale morphological filter. Multi-scale analysis is important to match the original signal properly. The unit SE is G(m) and the signal is S(n) as mentioned above where the scale is ϵ.

$\varepsilon = 1,2,....., \alpha$

The unit SE can be applied in this scale and mathematically will be represented below:

$$\varepsilon G(m) = G(m) \oplus G(m) \oplus .... \oplus G(m) \quad (6)$$

Multi-scale Dilation and Multi-scale Erosion will be represented below:

$$MD = (S \oplus \varepsilon G)(n) = S \oplus G \oplus .G \oplus .... \oplus G(n) \quad (7)$$

$$ME = (S\Theta\varepsilon G)(n) = S\Theta G\Theta.G\Theta..... .....\Theta G(n) \quad (8)$$

Further, the multi-scale gradient filter will be represented below:

$$G(n) = (S \oplus \varepsilon G)(n) - (S\Theta\varepsilon G)(n) \quad (9)$$

Structuring element is the main important part of morphological filters. The size and shape of the structuring element can be many types. The performance of the structuring element depends on the signal. The scale of any structuring element can be of two types, large and small. For noise suppression if the scale is large then the performance is better rather in case of preserving signal details the small scale is preferred. In most of the cases, the average value of the scales has been taken for better results and the mathematical equation is as follows.

$$G(n) = \frac{1`}{\lambda} \sum_{\varepsilon=1}^{\lambda} G_{\varepsilon}(n) \quad (10)$$

But all the scale should not take the same weight. Larger scale should take large weights for better performance and vice versa. In this work, an adaptive morphological filter has been proposed where a weight has been multiplied with the multi-scale morphological gradient filter. The equation of the adaptive morphological filter is given as:

$$AM(n) = \sum_{i=1}^{k} \omega_i G_i(n) \tag{11}$$

where $\sum_{i=1}^{k} \omega_i = 1$

Here, k is the scale number, ω_i is the weight coefficient, $G_i(n)$ is the ith output of the multi-scale morphological gradient filter. The output characteristic is directly influenced by this weighted method. These weights have to be optimized for better results. The WCA has been applied to determine the optimum combination of the weights. Here, the objective function is the mean square errors (MSRs) which are calculated from the actual and the filtered values.

A. Water Cycle Algorithm (WCA)

The WCA is created on the concept of the cyclical process of formation of rain drops from the evaporation of water which subsequently form streams that flow into the river and ultimately to the sea.

The streams are chosen as initial population with a matrix size of $(N_{pop} \times D)$, which are randomly generated from rain drops and they along with rivers move towards sea modifying their positions at each step. Thus

$$N_{popstream} = \begin{bmatrix} Stream_{Nsr}+1 \\ Stream_{Nsr}+2 \\ Stream_{Nsr}+3 \\ .... \\ .... \\ Stream_{Npop} \end{bmatrix} = \begin{bmatrix} x_1^1 & x_2^1 & x_3^1 & ..... & x_D^1 \\ x_1^2 & x_2^2 & x_3^2 & ..... & x_D^2 \\ ... & ... & ... & ... & ... \\ ... & ... & ... & ... & ... \\ ... & ... & ... & ... & ... \\ x_1^{Npop} & x_2^{Npop} & x_3^{Npop} & ..... & x_D^{Npop} \end{bmatrix} \tag{12}$$

The total number of populations N_{sr} ,however, comprises $N_{popstream} + N_{poprivers} + 1$ sea. For each river and the sea the following expression for NS_n streams hold:

$$NS_n = round\left\{ \left| \frac{Cost_n - Cost_{Nsr+1}}{\sum_{n-1}^{N_{sr}} C_n} \right| \times N_{streams} \right\} \tag{13}$$

where n=1, 2, 3....., N_{sr}

In the water cycle algorithm NS_n number of streams moves into the rivers and ultimately to sea. In the exploitation phase streams and rivers dynamically change their positions as:

$$\vec{X}_{stream}(t+1) = \vec{X}_{stream}(t) + rand \times C_1 \times \left(\vec{X}_{sea}(t) - \vec{X}_{stream}(t)\right) \tag{14}$$

$$\vec{X}_{stream}(t+1) = \vec{X}_{stream}(t) + rand \times C_1 \times \left(\vec{X}_{River}(t) - \vec{X}_{stream}(t)\right) \tag{15}$$

$$\vec{X}_{River}(t+1) = \vec{X}_{River}(t) + rand \times C_1 \times \left(\vec{X}_{sea}(t) - \vec{X}_{River}(t)\right) \tag{16}$$

Here *t* is the index of operations, optimal value of C_1 is 2 and $0 < C_1 < 2$ C .

If the stream exhibits a more optimal solution than its connecting river, then the positions of the particular river and the stream are exchanged and this happens in the same manner in case of river and sea.

Between a river and sea an evaporation operator used and that is represented as:

$$if \left\| \vec{X}_{Sea}^{t} - \vec{X}_{River}^{t} \right\| < d_{\max} \tag{17}$$

where rand<0.1 and j=1, 2, 3…., Nsr-1.

This operator is given to avoid premature convergence. Once evaporation is done, raining process starts and new streams are crated in various locations. New locations for the streams are created by uniform random search. The search intensity near the sea is controlled by d_{max}. The value of d_{max} adaptively reduced as given below:

$$d_{\max}(t+1) = d_{\max}(t) - \frac{d_{\max}(t)}{Max.Iteration} \tag{18}$$

$$t = 1,,2,3.....\ldots, Max\_Iteration$$

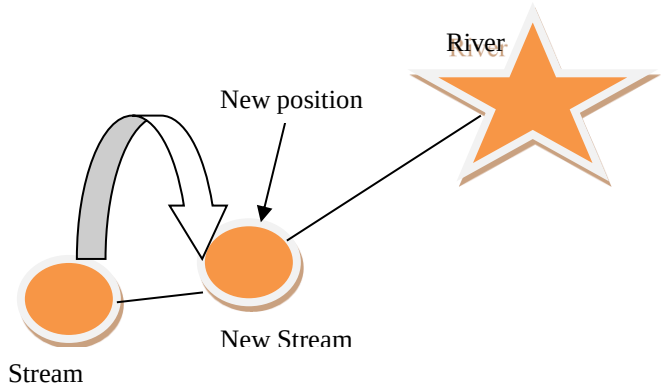

a. streams moving into a specific river

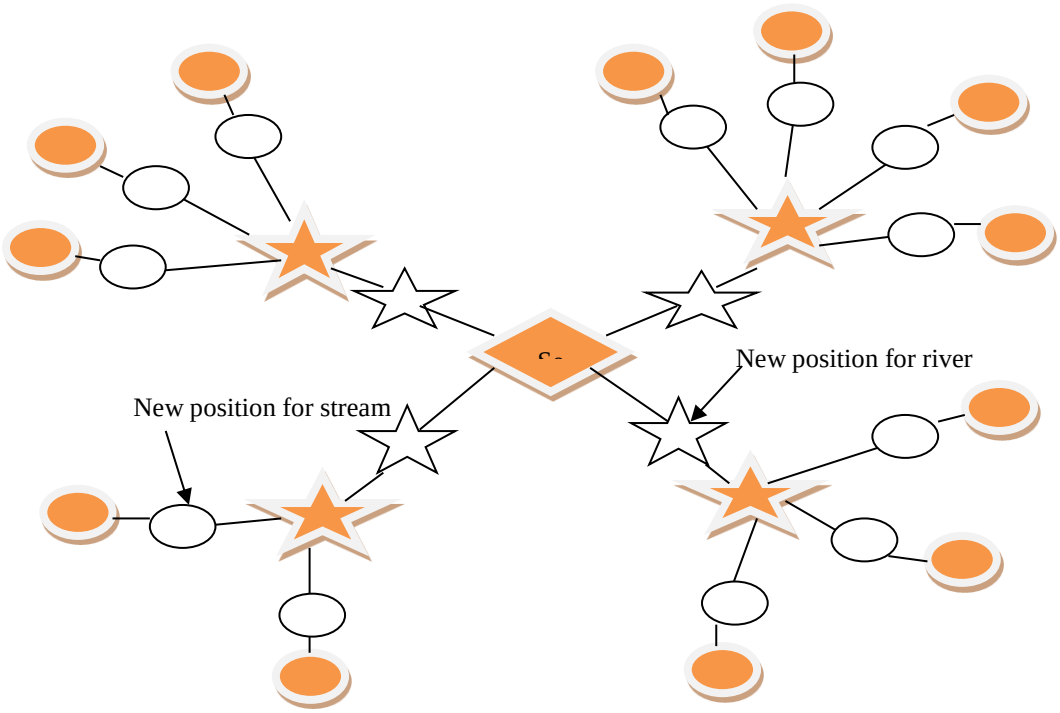

b. the water cycle algorithm

Figure 2. Schematic diagram

Figure 2a describes the schematic diagram of streams moving into the specific river and the diagram of the WCA has been given in Figure 2b. Figure 3 describes the convergence curve for AMF for weight optimization. Figure 4 describes the difference between the multi-scale morphological gradient filter and the proposed adaptive version of it. The islanding event has been taken for the consideration. One of the most important drawbacks of multi-scale morphological filter is that all the scales are having same weights. The adaptive version enhances the performance of MF which is clear from the Figure 4. In case of MF the amplitude of detection output of islanding event is small which overlap with other events such as load switching or sudden voltage drop. But in case of adaptive MF the amplitude threshold increases significantly. In noisy condition as well, the proposed AMF increases the performance. Two different types of PV penetration have been taken for the consideration.

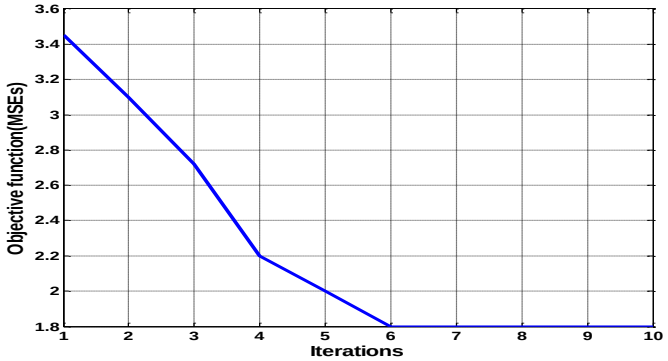

Figure 3. Water cycle convergence curve for adaptive multi-scale morphological filter for weight optimization

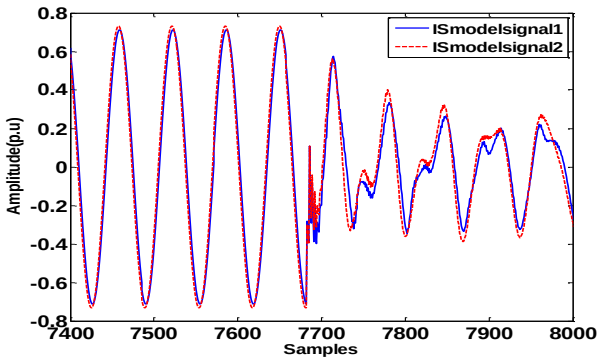

a. Model signal

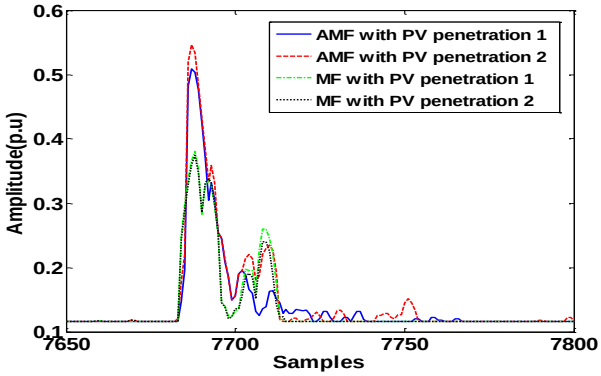

b. output of AMF

Figure 4. Comparative study of AMF with the normal MF over different PV penetrations

4. Feature Selection

In literature, there are many features that have been used for the classification of the disturbances. In this case, the features have been extracted from the output of the AMF. The features have to be significantly distinguishable so that the classification accuracy should be high. Classification accuracy will deteriorate if the features are not chosen properly. Here, five features are extracted after having a vast idea from the literature and the mathematical formulations of these features are given below.

P_1: energy of the output of AMF

P_2: mean value = $\sum_{n=-M}^{M} X_n \Big/ (2M+1)$ (19)

P_3: standard deviation = $\sqrt{\dfrac{\sum_{n=-M}^{M}(X_n - P_2)^2}{(2M+1)}}$ (20)

P_4: skewness = $\dfrac{\sum_{n=-M}^{M}(X_n - P_2)^3}{2M(P_3)^3}$ (21)

P_5: kurtosis = $\dfrac{\sum_{n=-M}^{M}(X_n - P_2)^4}{2M(P_3)^4}$ (22)

where X represents the output of AMF and M is the length of it.

5. Classification Using RRVFLN

A. Proposed Robust Regularized RVFLN (RRVFLN)

RVFLN is a single layer feed forward neural network where the hidden layer nodes are connected to the input nodes by a set of random weights and in addition there is a direct link between the input and output nodes. The weight vector β connecting the input and hidden layer nodes to the output layer is computed using generalized least squares. This simple structure produces fast convergence speed and generalization capability which are important for pattern classification. Mathematically the model of RVFLN is obtained as:

$$T(x) = \sum_{j=1}^{L} \beta_j h\left(w_j^T x + b_j\right) + \sum_{j=L+1}^{L+Z} \beta_j x_j \tag{23}$$

where the input data vector $x=[x_1, x_2, ..., x_Z]$; L represents the number of hidden layer nodes; w_j, b_j are random weight and bias vectors between the input and hidden layer nodes; Z is the total number of input nodes and T is the target vector and the total number of training samples is N, i=1, 2,....., N; β_j (j=1,2,.....,L) is the weight vector to be estimated.

The RRVFLN with l_2 norm is represented as:

$$\begin{aligned} &\min : J_1 = \frac{1}{2}\|\beta\|_2^2 + \frac{C}{2}\sum_{i=1}^{N}\xi_i^2 \\ &s.t : h(x_i)\beta = t_i - \xi_i \end{aligned} \tag{24}$$

where C is a regularization factor and $\sum_{i=1}^{N}\xi_i^2$ is the empirical loss and $\|\beta\|_2^2$ is the structural loss.

The regression performance of the regularized RVFLN deteriorates because of the availability of outliers and noise in the input data samples and a weighted RVFLN known as robust RRVFLN is formulated as

In this work, a robust regularized RVFLN (RRVFLN) has been suggested.

$$\min : \frac{1}{2}\|\beta\|_2^2 + \frac{C}{2}\sum_{i=1}^{N}\left\|w_i\xi_i\right\|_2^2$$
$$s.t : h(x_i)\beta = t_i - \xi_i \tag{25}$$

where the empirical loss weight is w_i of the i[th] sample. Using Karush-Kuhn-Tucker (KKT) theorem the modified cost function to be minimized is obtained as

$$J_{l2}(\beta,\xi,\alpha) = \frac{1}{2}\|\beta\|_2^2 + \frac{1}{2}C\sum_{i=1}^{N}(w_i\xi_i)^2 - \sum_{i=1}^{N}\alpha_i\left(h(x_i)\beta - t_i + \xi_i\right) \tag{26}$$

where α_i for the ith sample and for minimization the above equation is differentiated with respect to β, ξ and α, from which the value of β is obtained as

$$\beta = H^T\left(\frac{I}{C} + W^2HH^T\right)^{-1}W^2T$$

where

$$H = \begin{bmatrix} h(w_1,b_1,x_1) & .... & .... & h(w_L,b_L,x_1) & Z_1 \\ ... & .... & .... & ... & \\ ... & .... & .... & ... & \\ h(w_1,b_1,x_N) & .... & .... & h(w_L,b_L,x_N) & Z_N \end{bmatrix}_{N\times(L+Z)} \quad \beta = \begin{bmatrix} \beta_1 \\ ... \\ ... \\ \beta_{L+Z} \end{bmatrix}_{(L+Z)\times 1} \text{ and } \quad T = \begin{bmatrix} t_1 \\ ... \\ ... \\ t_N \end{bmatrix}_{N\times 1}$$

and

$$W^2 = diag[w_1^2, w_2^2, ..., w_N^2] \tag{27}$$

Here H is the hidden layer output matrix.

The weight matrix W is obtained by minimization of an objective function using maximum likelihood estimation based on based on Huber's algorithm. The objective function is given by

$$J(\beta_i) = \sum_{i=1}^{N}\rho(t_i) - \beta^T h(x_i) = \sum_{i=1}^{N}\rho(\xi_i) \tag{28}$$

Further, as per Huber to estimate the identifier's weight vector, k is specified (k is a positive number). Here k is called error or outlier threshold. The Huber's cost function is represented as: where ρ and W are obtained as

$$\rho(\xi_i) = \begin{cases} \frac{1}{2}\xi_i^2, & \left|\frac{\xi_i}{k}\right| \le 1 \\ k|\xi_i| - \frac{1}{2}k^2, & \left|\frac{\xi_i}{k}\right| > 1 \end{cases}, \quad W(\xi_i) = \begin{cases} 1, & \left|\frac{\xi_i}{k}\right| \le 1 \\ \frac{k}{|\xi_i|}, & \left|\frac{\xi_i}{k}\right| > 1 \end{cases} \tag{29}$$

and k is selected using Huber' concept as k=1.345 multiplied by MAR/0.6745;
MAR represents the absolute median error residual.

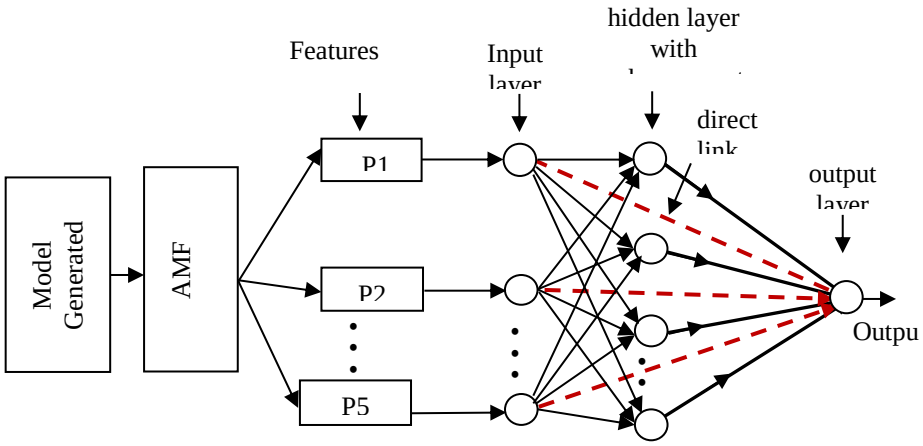

Figure 5a. Hybrid AMF and RRVFLN schematic diagram

Therefore for a sample input x_i the predicted output is obtained as:

$$O_i = h(x_i)\beta \tag{30}$$

6. Performance Evaluation using AMF based RRVFLN

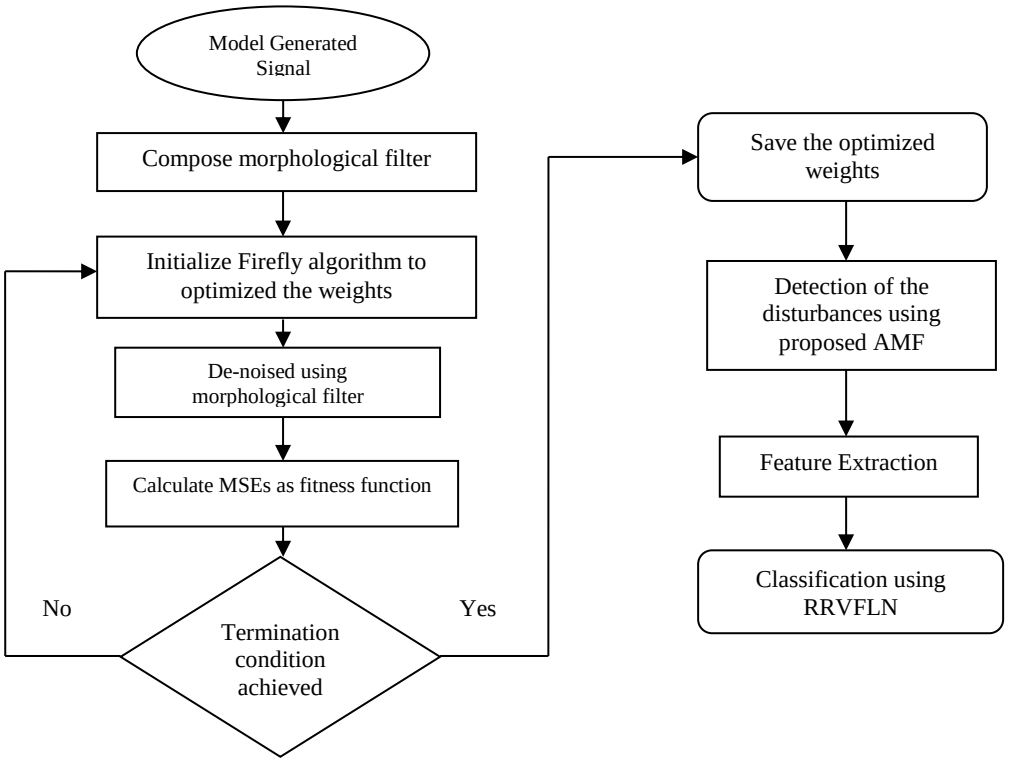

Figure 5b. Disturbances classification flow using AMF-RRVFLN

The three phase voltage signal samples are collected from a target DG terminal for an islanding event. However, there are multiple DGs present in the proposed microgrid model, so different islanding events can be created in different DG location. In the proposed microgrid model four PV systems have been used. The penetration of these PVs have been changed from the lower value to higher values to see how the output of AMF changes. In Figure 6 it has been found that the change of the AMF output is not much with different PV penetrations. Figure 7 represents the comparative study of AMF over MF in case of non detection zone where the threshold for AMF is much higher than the non detection zone threshold. Using the higher amplitude threshold the non detection zone has been reduced using proposed AMF.

Figure 8 describes the output of AMF for the LLL fault created in the microgrid model. Figure 9 describes the output of AMF for the capacitor switching in the microgrid model. With the extracted features the usefulness of the proposed AMF technique has been analyzed here. The model efficacy has been examined with the synthetic and model generated signals. The accuracy of the proposed AMF-RRVFLN has been tested, and also comparison is done with other recognized techniques.

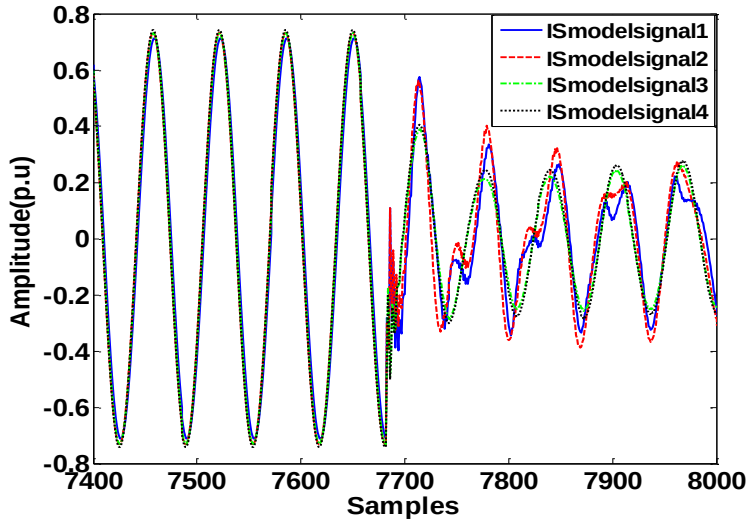

a. Model Signal

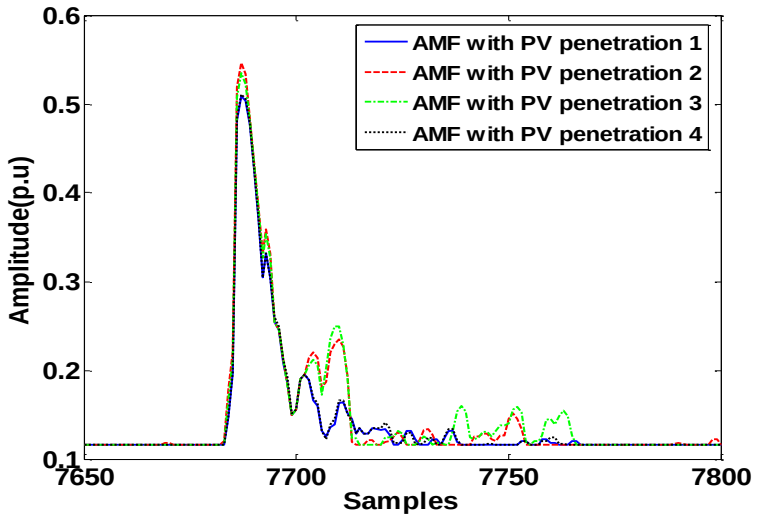

b. Output of the Proposed AMF

Figure 6. Threshold change with the proposed technique AMF in case of islanding event with different PV penetration

Total different 8 events were generated in the microgrid model. Total 1600 patterns were simulated for microgrid model generated different disturbances and 200 patterns were simulated for each event. Here 1200 patterns were taken for training the proposed RRVFLN. 1000 patterns are taken randomly for validation. The performance has been measured through accuracy (31). The Classification Accuracy (A_C) for a particular event 'a' can be represented as:

$$A_C(\%) = \frac{Number\ of\ \text{correctly classified patterns for a particular event 'a'}}{Number\ of\ \text{patterns of a particular event 'a'}} \times 100 \tag{31}$$

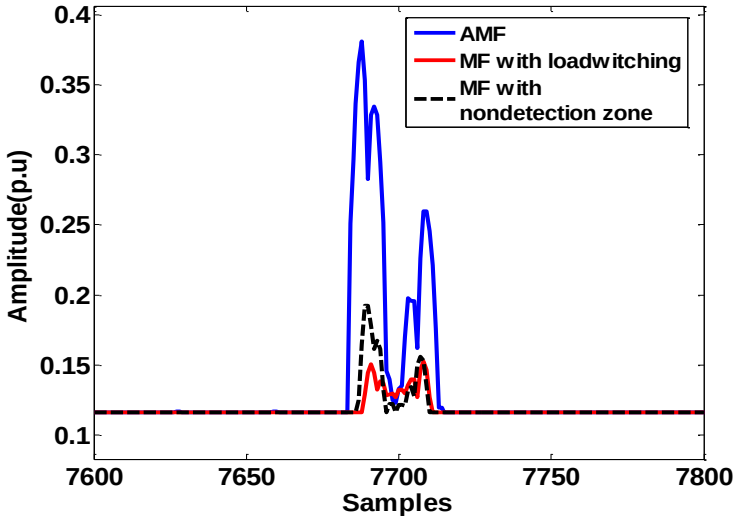

Figure 7. Comparative study of AMF with the normal MF in case of non detection zone

Table 3 represents the confusion matrix of AMF-RRVFLN in grid connected mode. The overall classification accuracy of the suggested method can be represented by confusion matrix, the correct class is shown by diagonal matrix. It is very clear from the confusion matrix that there is no miss classification for islanding event. Table 4 represents the classification accuracy of the proposed technique AMF based RRVFLN with different noisy conditions. The added white Gaussian noise with the microgrid generated signals is within 30db to 40db. The accuracy of the proposed method decreases with the increasing noise which is clear from Figure10. With 30db noise, the accuracy of the proposed method is 98.20% which is very much acceptable. At no noise condition the accuracy is 98.98% which is higher than many other recognized techniques with reduced detection time.

Table 3. Confusion Matrix of AMF-RRVFLN in grid-connected mode

Class	CI	CII	CIII	CIV	CV	CVI	CVII	CVIII
CI	200	0	0	0	0	0	0	0
CII	0	197	1	0	0	2	0	0
CIII	0	1	198	1	0	0	0	0
CIV	0	0	0	200	0	0	0	0
CV	0	0	0	0	198	0	1	1
CVI	0	1	0	0	1	197	0	1
CVII	0	1	0	0	1	1	197	0
CVIII	0	0	0	0	0	2	0	198

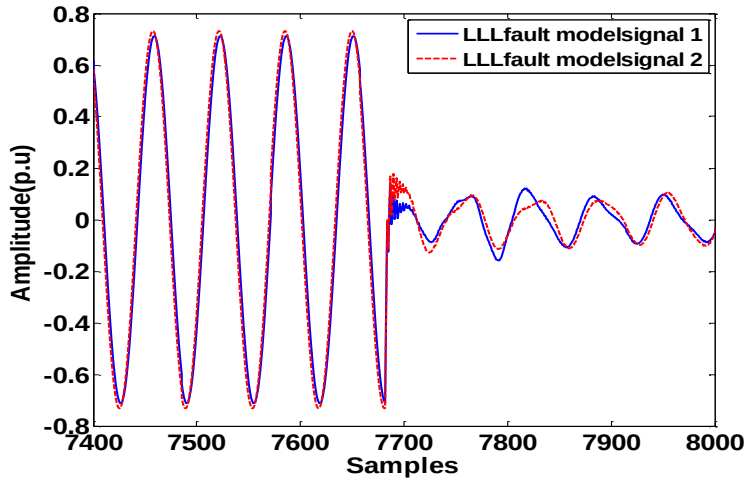

a. Model Signal

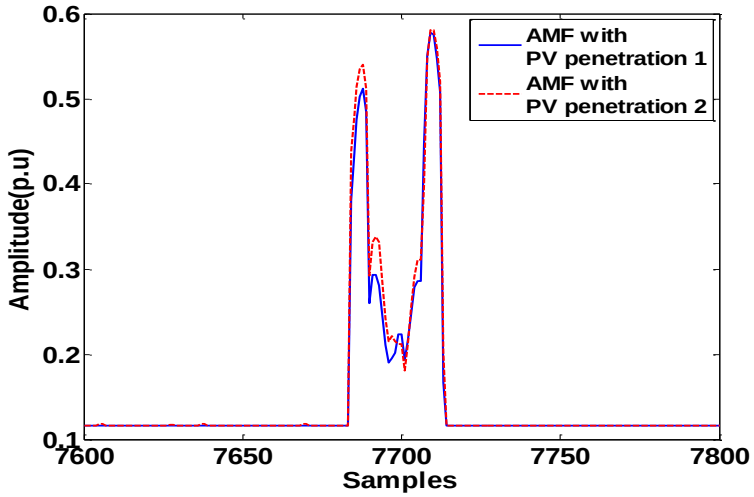

b. Output of The Proposed AMF

Figure 8. Threshold change with the proposed technique AMF in case of LLL fault event with different PV penetration

Table 4. Accuracy of AMF-RRVFLN in different noisy conditions in grid connected mode

Class	A_C (%) in AMF (no noise)	A_C (%) in AMF (30db noise)	A_C (%) in AMF (35db noise)	A_C (%) in AMF (40db noise)
CI	100	99.2	99.5	99.7
CII	98.71	98	98.22	98.53
CIII	99.12	98.52	98.75	99
CIV	99.3	98.79	98.89	99
CV	98.87	98.2	98.37	98.61
CVI	98.45	97.9	98	98.2
CVII	98.75	98	98.35	98.52
CVIII	98.67	97	97.29	98.5
Total	98.98	98.20	98.55	98.76

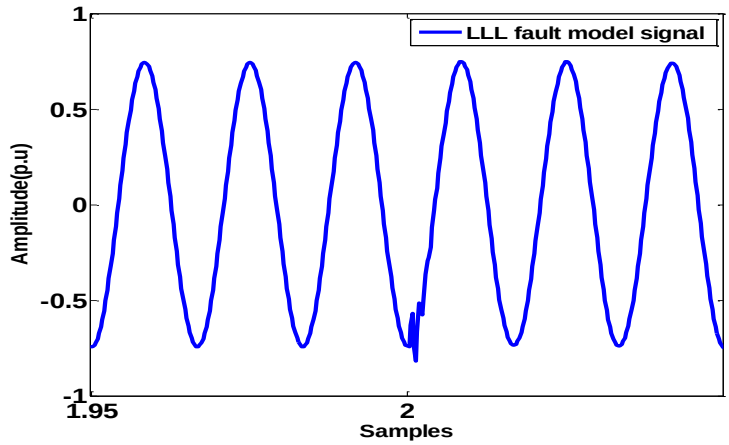

a. Model Signal

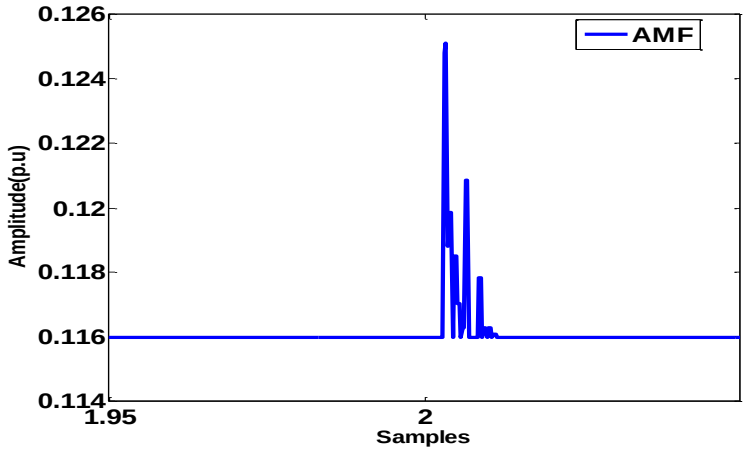

b. Output of The Proposed AMF

Figure 9. Threshold change with the proposed technique AMF in case of Capacitor Switching

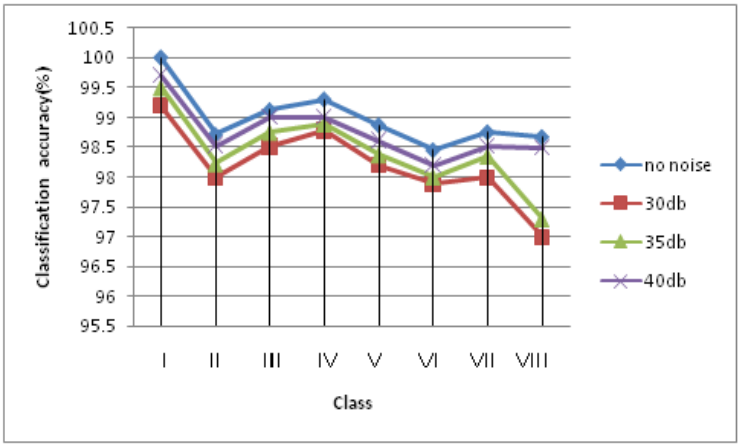

Figure 10. Classification accuracy of the proposed method for all the classes in different noisy conditions

Table 5. Average classification (%) accuracy of AMF over MF, WT, HHT under different noisy conditions

Techniques	without noise	30db noise	35db noise	40db noise
Average Classification accuracy of AMF	98.98	98.20	98.55	98.76
Average Classification accuracy of MF	98	97.33	97.67	97.8
Average Classification accuracy of WT	96.67	95.89	96	96.3
Average Classification accuracy of HHT	95.7	95	95.33	95.45

The average classification accuracy of the AMF technique is compared with other recognized methods such as normal MF, WT and HHT in different conditions like no noise, with noise (30 dB 35 dB, and 40 dB) and the results of which are displayed in Table 5. All the comparative results are given in Table 5 and Figure 11. It is found from numerical results shown in Table 5 that that the accuracy obtained in the AMF technique is higher than the others techniques in all the conditions. The AMF technique achieves with 98.98% classification accuracy in no noise condition which is superior to all other techniques like MF, WT and HHT where MF achieves 98%, WT achieves 96.67 and HHT achieves with 95.7% accuracy under no noise condition. Similarly in 30 dB noise condition the AMF exhibits the highest accuracy with 98.20%, in 35 dB noise condition it achieves with 98.55% whereas in 40 dB noise condition it achieves with 98.76% accuracy. For better visibility, the achieved average accuracies under different conditions are shown in Figure.11 which clearly indicates the supremacy of the AMF technique. HHT achieves the lowest average accuracy in all the conditions.

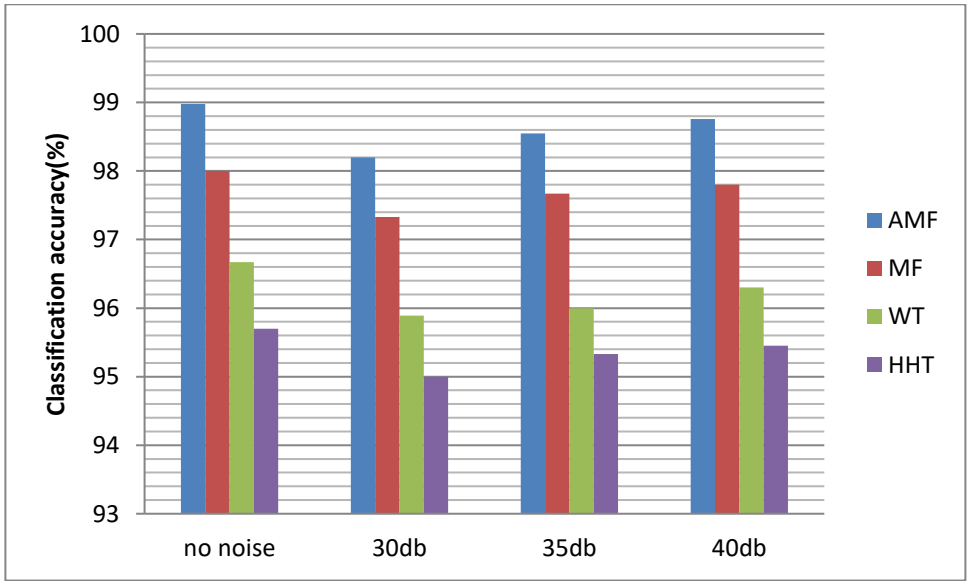

Figure 11. Classification accuracy (%) with different techniques in different noisy conditions

Some of the extracted feature values with different PV penetrations are given in Table 6 and Table 7 for Islanding and unbalanced load switching. Total five features were extracted for classification. The maximum amplitude and energy values of islanding and unbalanced load switching are given to show the threshold variations. The performance of the suggested classifier

RRVFLN has been compared with other classification techniques such as SVM and ELM and all the results are given in Table 8. Form Figure 12 it is clear that with AMF the classification accuracy is higher than ELM and SVM. Between ELM and SVM, the performance of ELM is better than SVM. Figure 13 describes the performance of MF with all three classifiers AMF, ELM and SVM, respectively. A comparative study has been done between AMF and MF to show the superiority of the proposed AMF. Table 9 represents the performance of the suggested method with other recognized methods which are also clear from Figure 14.

Table 6. Maximum amplitude for islanding and unbalanced load switching for different PV penetration

Class	PV1	PV2	PV3	PV4	Maximum Amplitude	Class	Maximum Amplitude
Islanding	100	100	100	100	0.0019	Unbalanced Load Switching	0.0136
	200	200	200	200	0.0019		0.0136
	200	100	400	200	0.0020		0.0136
	400	200	200	400	0.0021		0.0138
	400	400	400	400	0.0023		0.0138
	400	600	400	600	0.0023		0.0138
	600	600	600	600	0.0023		0.0141
	800	600	400	600	0.0025		0.0141
	800	800	600	600	0.0025		0.0141
	800	800	800	800	0.0025		0.0142
	1000	600	800	600	0.0026		0.0142
	1000	800	1000	800	0.0027		0.0143
	1000	1000	1000	1000	0.0027		0.0145

Table 7. Energy values for islanding and unbalanced load switching for different PV penetration

Class	PV1	PV2	PV3	PV4	Energy	Class	Energy
Islanding	100	100	100	100	0.5863	Unbalanced Load Switching	0.2674
	200	200	200	200	0.5863		0.2674
	200	100	400	200	0.5864		0.2675
	400	200	200	400	0.5865		0.2681
	400	400	400	400	0.5867		0.2682
	400	600	400	600	0.5867		0.2685
	600	600	600	600	0.5867		0.2688
	800	600	400	600	0.5875		0.2688
	800	800	600	600	0.5875		0.2690
	800	800	800	800	0.5875		0.2692
	1000	600	800	600	0.5881		0.2693
	1000	800	1000	800	0.5884		0.2695
	1000	1000	1000	1000	0.5888		0.2697

Table 8. Accuracy of AMF over MF with different classifier

	Classification Accuracy (%)					
Events	MF-SVM	AMF-SVM	MF-ELM	AMF-ELM	MF-RRVFLN	AMF-RRVFLN
CI	99	99	99.33	99.5	100	100
CII	97.33	98	97.89	98.33	98.33	98.71
CIII	97.67	98.33	98.25	98.75	98.67	99.12
CIV	97.89	98.67	98.5	99	98.75	99.3
CV	97.75	98.12	98.12	98.67	98.67	98.87
CVI	97.15	97.5	98	98	98.33	98.45
CVII	97	97.89	97.67	98.33	98.33	98.75
CVIII	96.85	97.97	97.23	98.25	98.15	98.67
Average Classification Accuracy	97.58	98.18	98.12	98.60	98.65	98.98

The classification accuracy achieved in the proposed AMF-RRVFLN is 100% for CI, 98.71% for CII, 99.12% for CIII, 99.3% for CIV. Class CV, CVI, CVII and CVIII achieves above 98% i.e. 98.87%, 98.45%, 98.75% and 98.67%, respectively. Altogether the achieved average accuracy is 98.98%. From the tabulated numerical results it is clear that among the different comparative methods like MF-SVM, AMF-SVM, MF-ELM, AMF-ELM, MF-RRVFLN, the proposed method achieves higher accuracy and overall higher average accuracy.

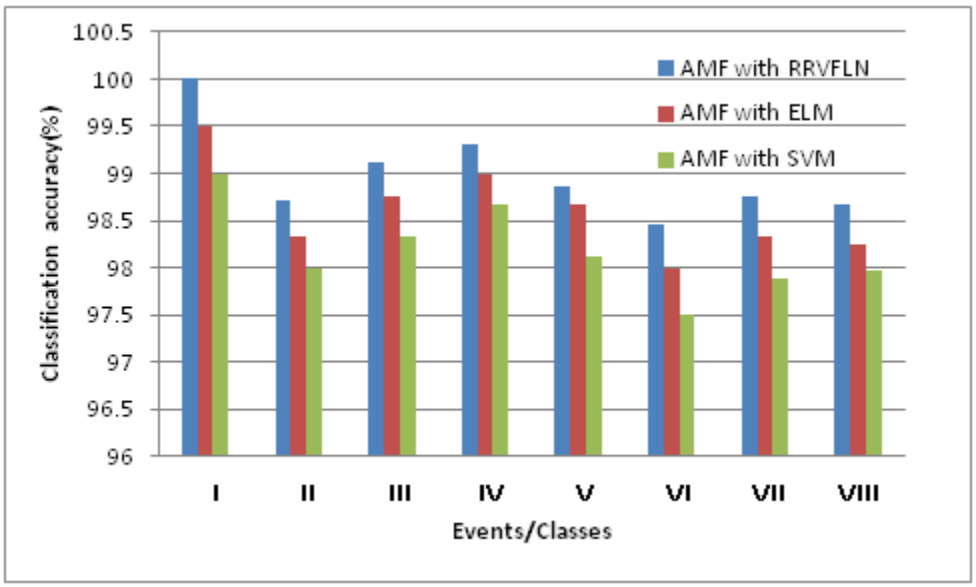

Figure 12. Average classification accuracy (%) of AMF with different classification techniques

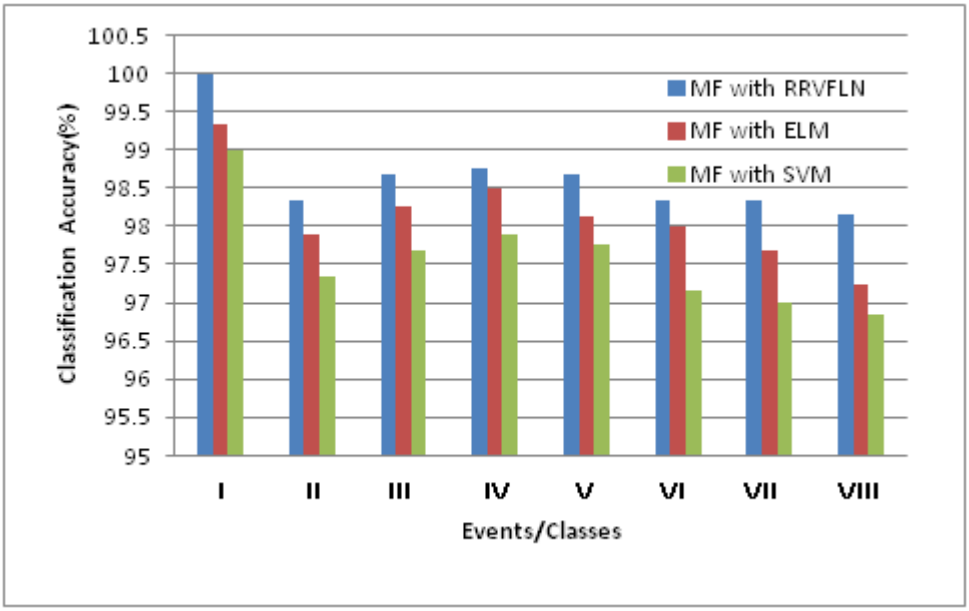

Figure 13. Average classification accuracy (%) of MF with different classification techniques

Table 9. Accuracy comparison of AMF-RRVFLN method with other recognized methods

Number	Different established methods	Classification Accuracy (%)
1	WT + fuzzy SVM	98
2	HHT + balanced neural tree	97.9
3	ST + PNN	97.4
4	WPD + SVM	97.25
5	WT + neural fuzzy	96.5
6	ST + modular NN	95.5
7	Proposed AMF + RRVFLN	98.98

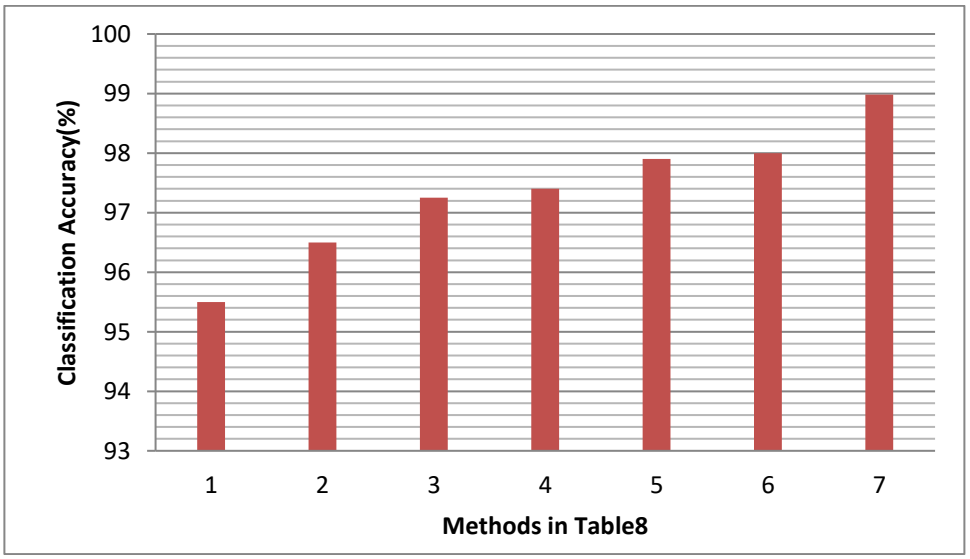

Figure 14. Classification Accuracy between different established methods

The most beneficial part of the proposed technique is that it takes less detection time compared to other established methods. Morphological filters are less complex than WT and ST. Table 10 describes the detection time for islanding with other existing methods where the proposed method takes only 21s for detection. The proposed method takes the lowest time and highest accuracy for islanding events as compared to the state-of-the-art methods mentioned in Table 10. Detection time taken by the proposed method for all other events is given in Table 11 where the maximum detection time is 26s for balanced and unbalanced load switching. The event capacitor switching and sudden voltage drop take 24s and 25s, respectively. The L fault, LL fault, and LLL fault take 23s, 22s and 21s, respectively. From the overall analysis and discussion it is concluded that the suggested method is an efficient method for classifying various PQ disturbances. This method is superior to many of the widely used existing methods.

Table 10. Time required for detection for islanding event with other recognized techniques

Recognized methods	Detection Time(ms)	Classification Accuracy (%)
Wavelet Transform[12]	25	97
Hybrid ST[12]	22	98.4
S-Transform[12]	26	97.2
Current and voltage harmonic distortion[38]	45	-
Current injection[38]	60	-
AMF (Proposed)	21	98.98

Table 11. Different events and its detection time in AMF

Events	Detection Time(ms)
Islanding (CI)	21
L fault (CII)	23
LL fault (CIII)	22
LLL fault (CIV)	21
Capacitor Switching (CV)	24
Unbalanced Load Switching (CVI)	26
Balanced Load Switching (CVII)	26
Sudden Voltage drop (CVIII)	25

PC Integrated Hardware in a loop based verification

For real-time implementation, a hardware set is utilized in order to capture various islanding and non-islanding disturbances including faults mixed with 30 dB white Gaussian noise with zero mean. The set up The microgrid disturbance signals are obtained through the high speed 12-bit analog to digital converter (ADC) known as DAQ USB-6008 device from National Instrument (NI) that provides multiple Analog Input-Output (AIO) and Digital Input-Output (DIO) channels with a full speed Analog Input (AI) sampling rate up to 10 kS/s. The firmware NI-DAQmx in MATLAB interface can capture the real-time disturbance signals via Serial Peripheral Interface (SPI) and host personal computer (PC). After training the PC interfaced hardware properly real time input disturbance signals comprising both the islanding and non-islanding events signals are observed by the Digital Output (DO) pins of NI USB-6008. Table 12 displays the classification accuracy obtained for different power quality disturbances signals.

It is noticed from the table that there are slight losses in the average accuracy (97.01%) as compared to the obtained average accuracy earlier in AM F-RRVFLN technique.

Table 12. Classification Accuracy obtained in AMF-RRVFLN in real-time

PQ disturbances	AMF-RRVFLN Accuracy
CI	97.65
CII	97.6
CIII	97.1
CIV	96.2
CV	97.15
CVI	96.45
CVII	96.85
CVIII	97.05
total	97.01

7. Conclusion

This work proposes an adaptive multiscale morphological filter (AMF) for extracting relevant features from a multi distribution generation based microgrid under both islanding and non-islanding disturbance conditions. The proposed multiscale morphological filter has better noise rejection property and retains the useful disturbance signal components in comparison to the traditional single scale morphological filter. Further it is made adaptive by a suitable choice of weighting factors by using the well known metaheuristic water cycle algorithm. For classification of both islanding and non-islanding events a fast, accurate randomized RVFLN classifier is used, which further has been made robust against the outliers if any in the signal data samples. The proposed combined AMF with RRVFLN has been verified for both the synthetic and Hardware in the loop based test system (DGs based distribution network) generated signals. The optimized morphological filter gives much better accuracy with reduced non detection zone which is a new idea contributed to literature. The classification accuracy (A_C) and the average classification accuracy of the suggested combined technique for both islanding and non-islanding events detection and classification are superior in comparison with other traditional methods.

8. References

[1]. Guo-Kiang Hung, Chih-Chang Chang, Chern-Lin Chen, "Automatic phase-shift method for islanding detection of grid-connected photovoltaic inverters", *IEEE Trans. on Energy Conversion*, vol.18, no.1, 2003,pp.169-173.

[2]. Badollah, K., Javad, S., "Islanding detection method for photovoltaic distributed generation based on voltage drifting', *IET Gener. Transm. Distrib*., vol.7, 2013, pp. 584–592.

[3]. Jang, S., Kim, K.,"An islanding detection method for distributed generation using voltage unbalance and total harmonic distortion of current", *IEEE Trans. Power Delivery*, vol. 19, 2004, pp. 745–75217

[4]. Zeineldin, H.H., Conti, S., "Sandia frequency shift parameter selection for multiinverter systems to eliminate non-detection zone", *IET Renew. Power Gener*., vol. 5, 2011, pp. 175–183.

[5]. Wang, X., Freitas, W., Xu, W.,et. al., "Impact of DG interface controls on the Sandia frequency shift antiislanding method", *IEEE Trans. Energy Convers*., vol. 22, no.3, 2007 pp. 792–794.

[6]. Byeong-Heon, K., Seung-Ki, S., Chun-Ho, L., "Anti-islanding detection method using negative sequence voltage". *Int. Conf. Power Electronics and Motion Control*, 2012, pp. 604–608.

[7]. K Jia, H Wei, T Bi, DWP Thomas, "An islanding detection method for multi-DG systems based on high-frequency impedance estimation", *IEEE Trans. on Sustainable energy*, vol.8, no.1, 2017, pp.74-83.

[8]. H. Samet, F. Hashemi, and T. Ghanbari, "Islanding detection method for inverter-based distributed generation with negligible non-detection zone using energy of rate of change of voltage phase angle", *IETGener., Transmiss. Distrib*., vol. 9, no. 15, Jul.2015, pp. 2337–2350.

[9]. X. L. Chen and Y. L. Li, "An islanding detection algorithm for inverter-based distributed generation based on reactive power control," *IEEE Trans. Power Electron*.,vol. 29, no. 9, 2014, pp. 4672–4683'

[10]. J. Zhang, D. H. Xu, G. Shen, Y. Zhu, N. He, and J. Ma, "An improved islanding detection method for a grid-connected inverter with intermittent bilateral reactive power variation," *IEEE Trans. Power Electron*., vol. 28, no. 1, 2013, pp. 268–278.

[11]. Karimi, H., Yazdani, A., Iravani, R.,"Negative-sequence current injection for fast islanding detection of a distributed resource unit", *IEEE Trans. Power Electronics*, vol. 23, 2008, pp. 298–307.

[12]. Dhar, Snehamoy, and Pradipta Kishore Dash, "Adaptive threshold based new active islanding protection scheme for multiple PV based microgrid application", *IET Generation, Transmission & Distribution*, vol.11, no. 1, 2017, pp. 118-132.

[13]. G. H. Gonzalez and R. Iravani, "Current injection for active islanding detection of electronically-interfaced distributed resources", *IEEE Trans. Power Del*., vol. 21, no. 3, 2006, pp. 1698–1705.

[14]. Ankita Samui and S. R. Samantaray, "Assessment of ROCPAD Relay for Islanding Detection in Distributed Generation", *IEEE Trans. on Smart Grid*, vol.2, no.2, 2011, pp.391-398.

[15]. Mohanty, S.R., Kishor, N., Ray, P.K.,et al.,"Comparative study of advanced signal processing techniques for islanding detection in a hybrid distributed generation system", *IEEE Trans. Sustain. Energy*, vol. 6, 2014, pp. 122–131.

[16]. PK Dash, SK Barik, RK Patnaik, "Detection and classification of islanding and nonislanding events in distributed generation based on fuzzy decision tree", *Journal of Control, Automation and Electrical Systems*, vol. 25, no.6 , 2014, pp.699-719.

[17]. Hsieh, C., Lin, J., Huang, S., "Enhancement of islanding-detection of distributed generation systems via wavelet transform-based approaches", *Electr. Powe and Energy Syst*., 2008, vol. 30, pp. 575–580.

[18]. P. K. Ray, Nand Kishor, and S. R. Mohanty, "Islanding and Power Quality Disturbance Detection in Grid-Connected Hybrid Power System Using Wavelet and –Transform," *IEEE Trans. on Smart Grid*, vol.3, no.3, 2012, pp.1082-1094.

[19]. Chakravorti, Tatiana, Rajesh Kumar Patnaik, and Pradipta Kishore Dash, "Detection and classification of islanding and power quality disturbances in microgrid using hybrid signal processing and data mining techniques", *IET Signal Processing*, vol.12, no. 1, 2017, pp. 82-94.

[20]. Dionisis Voglitsis, Nick Peter Papanikolaou, and Anastasios Ch. Kyritsis, " Active Cross-Correlation Anti-Islanding Scheme for PV Module-Integrated Converters in the Prospect of High Penetration Levels and Weak Grid Conditions", *IEEE Trans. on Power Electronics*,vol. 34, no. 3, 2019, pp. 2258-2274.

[21]. Dash, P., Tatiana Chakravorti, and R. Patnaik, "Advanced signal processing techniques for multiclass disturbance detection and classification in microgrids", *IET Science, Measurement and Technology*, vol.11, no.4,2017, pp. .504-515.

[22]. Hieu Thanh Do, Xing Zhang, Ngu Viet Nguyen, Shan Shou Li, and Tho Thi-Thanh Chu, " Passive-Islanding Detection Method Using the Wavelet Packet Transform in Grid-Connected Photovoltaic Systems", *IEEE Trans. on Power Electronics*, vol.31, no.10, 2016, pp.6955-6967.

[23]. Omar N. Faqhruldin, Ehab F. El-Saadany, and Hatem H. Zeineldin, "A Universal Islanding Detection Technique for Distributed Generation Using Pattern Recognition", *IEEE Trans. on Smart Grid*, vol.5, no.4, 2014, pp.1985-1992.
[24]. Achlerkar, Pankaj D., Subhransu R. Samantaray, and M. Sabarimalai Manikandan, "Variational Mode Decomposition and Decision Tree Based Detection and Classification of Power Quality Disturbances in Grid-Connected Distributed Generation System", *IEEE Transactions on Smart Grid*, vol.9, no.4, 2018, pp.3122-3132.
[25]. Mrutyunjaya Sahani, and Pradipta Kishore Dash, "FPGA-Based Online Power Quality Disturbances Monitoring Using Reduced-Sample HHT and Class-Specific Weighted RVFLN", *IEEE Trans. on Industrial informatics*, vol.15, no.8, 2019, pp.4614-4623.
[26]. Musliyarakath Aneesa Farhan1, Shanti Swarup K, " Mathematical morphology-based islanding detection for distributed generation", *IET Gen., Trans.& Dist.*, vol.11, no.14, 2017, pp.3449-3457.
[27]. Y. Li, X. Liang, and M. J. Zuo, "A new strategy of using a time varying structure element for mathematical morphological filtering," *Measurement*, vol. 106, pp. 53–65, 2017.
[28]. C. Li, M. Liang, Y. Zhang, and S. Hou, "Multi-scale autocorrelation via morphological wavelet slices for rolling element bearing fault diagnosis," *Mechanical Systems and Signal Processing*, vol. 31, pp. 428–446, 2012.
[29]. Y. Dong, M. Liao, X. Zhang, and F. Wang, "Faults diagnosis of rolling element bearings based on modified morphological method," *Mechanical Systems and Signal Processing*, vol. 25, no. 4, pp. 1276–1286, 2011.
[30]. Y. Li, X. Liang, J. Lin, Y. Chen, and J. Liu, "Train axle bearing fault detection using a feature selection scheme based multiscale morphological filter," *Mechanical Systems and Signal Processing*, vol. 101, pp. 435–448, 2018.
[31]. Y. Zhang, J. Wu, Z. Cai, B. Du, P. S. Yu, "An unsupervised parameter learning model for RVFL neural network", Neural Networks, vol. 112 , 2019, pp. 85- 97.
[32]. R. Katuwal, P. N. Suganthan, "Enhancing multi-class classification of random forest using random vector functional neural network and oblique decision surfaces", in: 2018 *International Joint Conference on Neural Networks (IJCNN)*, 2018, pp. 1-8.
[33]. Y. Ren, P. N. Suganthan, N. Srikanth, G. Amaratunga, "Random vector functional link network for short-term electricity load demand forecasting", Information Sciences, vol. 367-368, 2016, pp. 1078 {1093.
[34]. L. Zhang, P. N. Suganthan, "A comprehensive evaluation of random vector functional link networks", Information Sciences, vol. 367-368, 2016, pp. 1094-1105.
[35]. Sadollah, A., Eskandar, H., Bahreininejad, A. and Kim, J.H., " Water cycle algorithm with evaporation rate for solving constrained and unconstrained optimization problems", Applied Soft Computing, vol.30, 2015, pp.58-71.
[36]. Eskandar, H., Sadollah, A., Bahreininejad, A. and Hamdi, M., "Water cycle algorithm–A novel metaheuristic optimization method for solving constrained engineering optimization problems", Computers & Structures, vol. 110, 2012, pp.151-166.
[37]. Sadollah, A., Eskandar, H. and Kim, J.H., 2015. "Water cycle algorithm for solving constrained multi-objective optimization problems", Applied Soft Computing, vol.27, 2015, pp.279-298.
[38]. Mahela, Om Prakash, Abdul Gafoor Shaik, and Neeraj Gupta. "A critical review of detection and classification of power quality events." Renewable and Sustainable Energy Reviews, vol. 41, 2015, pp. 495-505.
[39]. Singh, Shubhendra Pratap, Abdul Hamid Bhat, and Arfat Firdous. "A Novel Reduced-Rule Fuzzy Logic Based Self-Supported Dynamic Voltage Restorer for Mitigating Diverse Power Quality Problems." *International Journal on Electrical Engineering and Informatics* 11, no. 1 (2019): 51-79.
[40]. Sandhu, Kanwarjit Singh, and Aeidapu Mahesh. "Optimal sizing of PV/wind/battery Hybrid Renewable Energy System Considering Demand Side Management." *International Journal on Electrical Engineering and Informatics* 10, no. 1 (2018): 79-93.

[41]. Kumar, Pradeep. "Comparative Power Quality analysis of Conventional and Modified DSTATCOM Topology." *International Journal on Electrical Engineering and Informatics* 9, no. 4 (2017): 786-799.
[42]. Prakash, D., R. Mahalakshmi, and M. Karpagam. "Power Quality Enhancement in STATCOM connected Distribution Systems based on Gravitational Search Algorithm." *International Journal on Electrical Engineering & Informatics* 8, no. 4 (2016).
[43]. Sundarabalan, C. K., and K. Selvi. "Power quality enhancement in power distribution system using artificial intelligence based dynamic voltage restorer." *International Journal on Electrical Engineering and Informatics* 5, no. 4 (2013): 433.

N. R. Nayak received his B. Eng. in electronics and telecommunication from Utkal University, India in 1992, the M. Eng. degree in communication system engineering from Biju Patnaik University of Technology, India in 2004, and continuing his Ph. D. in Siksha "O" Anusandhan Deemed to be University, India.
He is currently the director of Microsys Infotech, India. His research interests include signal processing, pattern recognition and classification.
nihar.microsys@gmail.com. ORCID iD: 0000-0002-1524-7837

P. K. Dash received the M. Eng. degree in electrical engineering from Indian Institute of Science, India in 1964, the Ph. D. degree in electrical engineering from the Sambalpur University, India in 1972, and the Doctoral of Science (D.Sc.) degree in electrical engineering from the Utkal University, India in 2003.
He is currently director of research in the Multidisciplinary Research Cell of the Siksha "O" Anusandhan University, India. He has published more than 500 papers in international journals and conferences. His research interests include renewable energy, micro and smart grid, machine intelligence, signal processing and control, power quality, etc.
pkdash.india@gmail.com (Corresponding author), ORCID iD: 0000-0002-8950-7136

B. N. Sahu received his B. Tech. degree in Electronics and Telecommunication from Utkal University, India in 1997, M. Tech. degree in Communication System engineering from Biju Patnaik University of Technology, India in 2004, and Ph. D. degree from Siksha "O" Anusandhan University, Odisha, India in 2015. His
research interests include signal processing, system identification, classification, pattern recognition etc.
badrinarayansahu@soa.ac.in

Ranjeeta Bisoi received the M.C.A. degree from North Orissa University, India in 2011, and the Ph. D. degrees in computer engineering from Siksha "O" anusandhan University, India 2015. She is currently working as a Resacrh Asst. Professor in the Multidisciplinary Research Cell of Siksha "O" Anusandhan
University, India. She has published 40 papers in international journals and conferences. Her research interests include soft computing, data mining, machine intelligence and bioinformatics.
ranjeeta.bisoi@gmail.com. ORCID iD: 0000-0002-2651-2130